JOURNAL OF APPLIED ELECTROCHEMISTRY 5 (1975) 145–150

Application of Electron Spectroscopy for Chemical Analysis (ESCA) to the study of iron-based battery electrodes

I. OLEFJORD

Department of Engineering Metals, Chalmers University of Technology, Fack, S–40220 Göteborg, Sweden

Received 15 July 1974

Electron Spectroscopy for Chemical Analysis (ESCA) has been used in combination with X–ray diffraction (XRD) and energy-dispersive X–ray analysis (EDAX) to study the oxidation state, structure and morpholog of pure iron and iron-cadmium electrodes in various stages of cycling. The electrodes have only been studied in their discharged state. Cycling produces particle coarsening and a change in phase composition of the iron compounds from Fe_3O_4 to α–Fe. ESCA spectra suggest that a thin cadmium-rich surface film of poor electronic conductivity forms on the surface of the particles after prolonged cycling.

1. Introduction

The iron electrode, although technically established for a long time, has received very little study with modern physical methods. ESCA [1] appears particularly interesting in this connection because of its ability to identify the valence state of each atomic species in the specimen and because of its sensitivity to very thin surface films.

This report describes a preliminary study intended to probe the potential of ESCA (in combination with conventional X–ray diffraction and scanning electron microscopy) for research in the field of secondary electrodes. Changes that occur in various stages of the cycling life have been followed. The study is restricted to the fully discharged state of the electrodes.

2. Experimental

Experimental electrodes were made up of an iron-magnetite powder to which about 8% CdO powder was added. 3 g of the ground mixture were encapsulated in electrode pockets of perforated iron foil in accordance with normal procedure in battery manufacture. After soaking in KOH, the electrodes were formed by cyclic charging and discharging in new electrolyte. Thereafter, they were cycled automatically with 5 h charging and 3 h discharging times at 150 mA. The electrolyte used was KOH with a specific weight of $1{\cdot}25\,l^{-1}\,cm^{-3}$. To this, 20 mg of Li had been added. The cell capacity was measured at regular intervals by determining the time needed to discharge the electrode to −800 mV versus a saturated Hg/HgO reference electrode at a current of 140 mA. Normally, the electrolyte was protected against pick-up of carbon dioxide from the air by a plastic film. In a few experiments, the electrolyte was unprotected.

Before study by XRD, SEM and ESCA, all electrodes were discharged to 0 V versus Hg/HgO, removed from the cell and soaked in water and methanol, and finally dried in air at 40°C. The electrodes were cooled with liquid nitrogen and fractured to expose undisturbed cross sections of the electrode mass for investigation by scanning microscopy. Samples for XRD and ESCA were taken in the form of powder from the whole cross section.

3. X-ray diffraction analysis (XRD)

The crystallographic phase composition of the electrode material was studied in the unformed state and after various numbers of cycles, using Co Kα radiation. Fig. 7 shows diffractograms obtained in the unformed state (top) and at the end of the cycling life (bottom). The intensities of characteristic peaks of the various crystal phases at different fractions of the cycling life are compiled in Table 1.

The virgin mass consists of α—Fe, Fe_3O_4 and CdO. Cycling decreases the ratio of Fe_3O_4 to α—Fe until at the end of the cycling Fe_3O_4 is no longer detectable (Fig. 7).

Cadmium oxide disappears from the diffractogram after formation and early cycling. After 6 cycles, very weak diffraction peaks $Cd(OH)_2$ are present. Prolonged cycling increased the intensity of $Cd(OH)_2$, and its intensity ratio to α—Fe remained roughly constant during the cycling life. An exception is noted for two electrodes which were cycled in open cells, with the electrolyte exposed to air (40 and 80 cycles, cf. Table 1). X—ray diffraction showed a small amount of $CdCO_3$ after 40 cycles, and about twice as much after 80 cycles. At the same time, the diffraction peak of $Cd(OH)_2$ was reduced. Weak diffraction peaks of metallic cadmium are present after 180 cycles and after 80 cycles for the unprotected electrode. A precipitate of Li_2CO_3 had formed on the outside of the electrode plate [2] although no Li_2CO_3 could be detected inside.

4. Scanning electron microscopy (SEM)

Fig. 1 shows the structure of the compacted electrode mass before formation. At lower magnification, it can be seen that the particles of the powder blend are lumped together into fairly large aggregates. The size of the powder particles or aggregates is not changed during formation and early cycling. Fig. 2 shows the structure of a fracture surface after 6 cycles.

The main structural change observed during cycling is a coarsening of the powder particles. In the unformed state and after initial cycling, the particle size is about 0·3 μm; after 40 cycles in an open cell it has grown to about 0·5 μm, but there are regions of much coarser particle size near the electrode surfaces (Fig. 3). In protected cells, particle growth is not quite so pronounced. Fig. 5 shows, after 180 cycles in a protected cell, an average particle size of about 1 – 2 μm. Spot analysis with an energy-dispersive X—ray analyzer (EDAX) of the larger particles in electrodes cycled under protection for 100 and 180 cycles showed these particles to contain mainly iron.

The large particles formed in electrodes that had been cycled without protection were found to contain both iron and cadmium. Their large size (up to 10 μm as shown in Fig. 4) allowed a more reliable analysis which gave a peak ratio of FeKα:CdLα = 5·9:1 in the large particles of trigonal habit, while the fine-grained regions showed FeKα:CdLα = 13·3:1. The average ratio over a large area containing both types of component was 8·1:1.

5. Electron Spectroscopy for Chemical Analysis (ESCA)

While EDAX allows spot analysis of the chemical composition of individual particles, it is not sensitive to very thin surface coatings. ESCA, on the other hand, has high sensitivity for thin surface films (it 'sees' only the top 2 – 4 nm of the specimen) but cannot be focussed on any individual particle. The physical principle of the method has been described by its author, K. Siegbahn [1]. Basically, one analyzes the photoelectrons excited from the specimen surface by X—ray bombardment; their kinetic energy reflects the binding energy of the electrons in the atoms near the specimen surface and thus can reveal both their chemical identity and valence state.

The ESCA instrument employed in this study was a Hewlett Packard 5950 A, equipped with a special specimen handling system that has been described elsewhere [3]. An important feature of the handling system in the present connection is the possibility to strip away successive portions of surface material by ion bombardment, which extends the applicability of the method to greater depths below the original surface, or allows one to remove oxidation products and adsorbates formed during contact of the specimen with the atmosphere.

Positive ionization produces a 'chemical shift' of the ESCA peaks in the direction of higher binding energy, which can be used to identify the valence state of the metal atoms. Negative ionization in anions produces a chemical shift in the opposite direction. Fig. 8 shows typical spectra of electrons from the $2p_{3/2}$ orbital of iron in the divalent and the three-valent state in synthetic Fe_3O_4. (In the Fe_3O_4 spectrum shown, the intensity of the Fe^{++} peak

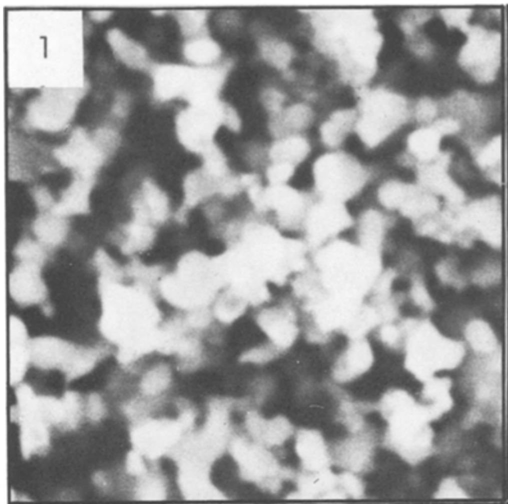

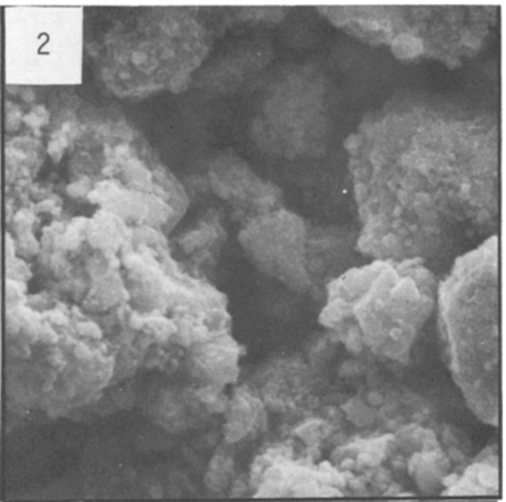

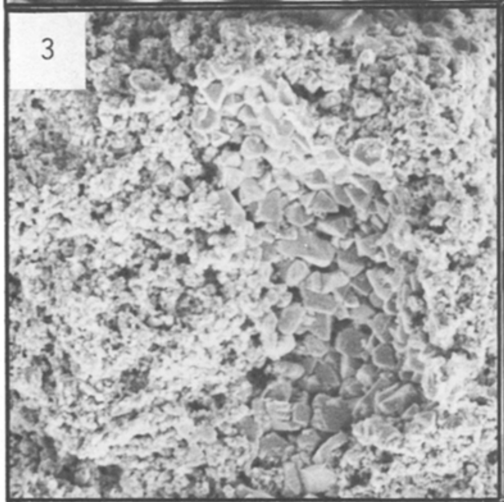

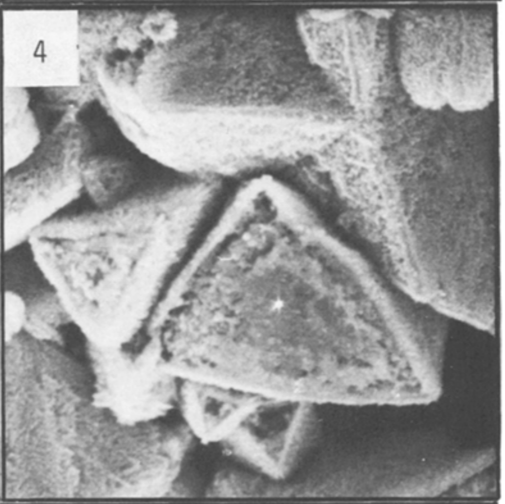

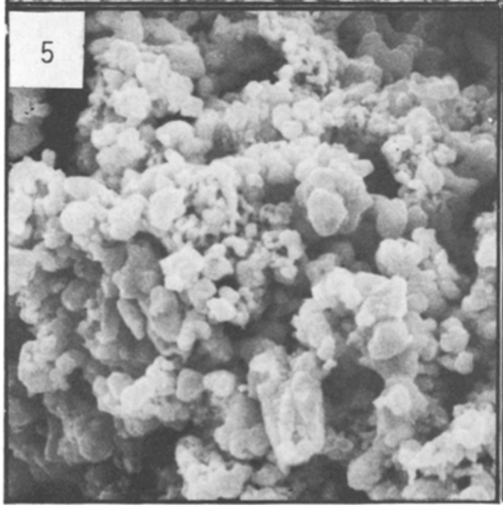

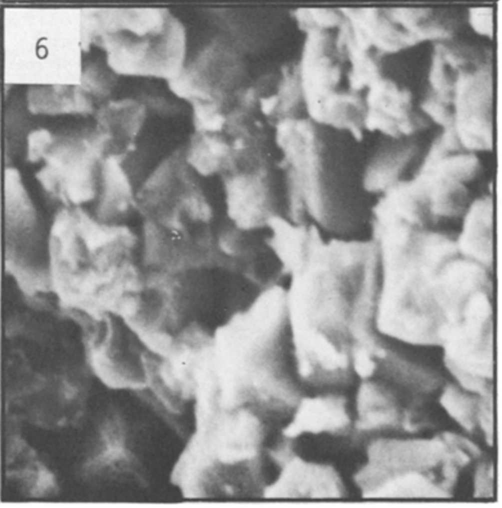

Figs. 1 – 5. Cd – containing electrode. Fig. 1: uncycled, × 10 000; Fig. 2: cycled 6 times, × 3000; Fig. 3: cycled 40 times, × 300; Fig. 4: cycled 40 times, × 3000; Fig. 5: cycled 180 times, × 3000. Fig. 6. Cd–free electrode, cycled 100 times, × 3000.

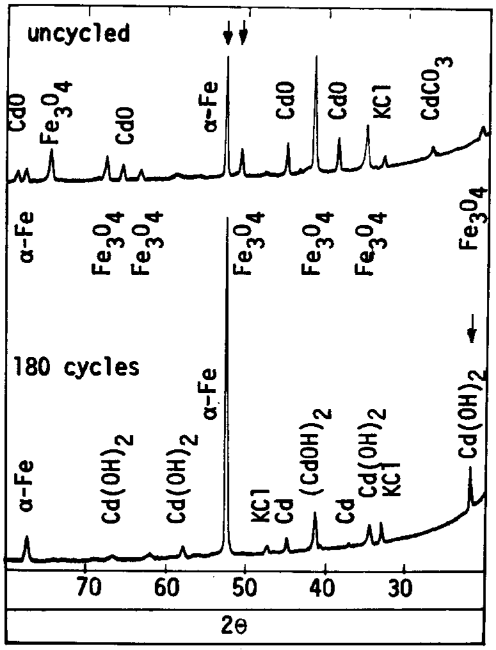

Fig. 7. X–ray diffraction pattern obtained in the unformed state (top) and after 180 cycles (bottom). The diffraction peaks marked by arrows, α—Fe (1 0 0). Fe_3O_4 (4 0 0) and $Cd(OH)_2$ (0 0 1), have been used in Table 1.

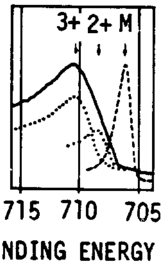

Fig. 8. ESCA spectra of Fe $2p_{3/2}$ level of Fe_3O_4 (solid line) and metallic Fe (dashed line). The dotted lines show an approximate deconvolution of the oxidized peak in its divalent and trivalent components.

is somewhat lower than expected, owing to superficial oxidation to Fe^{+++}). The dashed peak corresponds to the metallic state of iron.

In interpreting ESCA spectra, one has to distinguish true chemical shifts from shifts produced by changes in the electrical potential of the specimen surface. Such changes, which can occur in poorly conducting specimens owing to unbalance between loss of photoelectrons and pick-up of stray electrons at the isolated surface, will shift all the peaks in a spectrum uniformly. Chemical shifts, on the other hand, affect the peaks of each element in a specific manner. Since some of the compounds occurring in electrode masses – notably hydroxides - are poor conductors, we must be prepared to encounter such 'surface potential' shifts (S.P. shifts) in the present material.

The specimens were prepared by grinding the electrode masses to a fine powder in pure alcohol and letting a drop of the slurry evaporate on a gold-plated ESCA specimen holder. Fig. 9 shows sections of the ESCA spectra in the energy ranges where characteristic peaks of Fe, Cd and O occur. The absolute intensity above background is stated beside each peak. Ion etching was performed on all specimens, but produced changes only in the case of the freshly formed electrode (6 cycles). The spectrum obtained before ion etching is indicated by dotted lines.

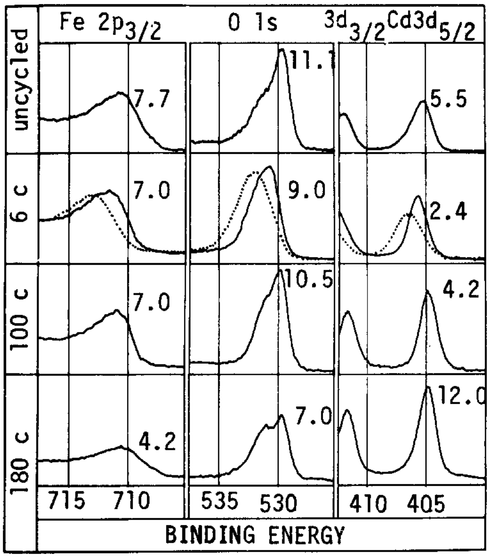

Fig. 9. ESCA spectra of the Cd containing electrode mass after various numbers of cycles. The figures beside each peak show the intensity above background in K counts s^{-1}. The dotted peaks in row 2 are the spectra recorded before ion etching.

The ESCA spectrum of the unformed electrode mass indicates that iron is present mainly in the three valent state, suggesting considerable surface oxidation of both the Fe_3O_4 and the α—Fe which are known to be present from the X–ray diffraction results. Also the Cd peak agrees with that of a reference spectrum of CdO, indicating that Cd is present in the fully oxidized state. Finally, the position of the oxygen peak is the normal one for anionic oxygen.

Turning to the spectrum of the freshly formed electrode (6 cycles) we find all peaks shifted towards higher binding energy (lower kinetic energy) before ion milling. Ion milling restores them to positions similar to those in the unformed state. The integrated peak intensities remain roughly constant during ion etching. Compared to the unformed state, the intensity ratio of Fe:O is unchanged, but that of Cd:Fe is reduced. We know from the XRD results that CdO is dissolved while diffuse $Cd(OH)_2$ peaks appear at the very limit of detectability. The SEM pictures indicate that any hydroxide precipitation must be on a very fine scale or in the form of a thin film on the original particles of the powder mass because the overall morphology is not changed.

One could assume that a thin overlay of hydroxide or a noncrystalline precipitate covered the iron particles before ion etching. ESCA studies of pure CdO and $Cd(OH)_2$ show negligible S.P. shifts in the former but strong ones in the latter. This might explain the general shift of the peaks towards higher binding energies before ion milling. Superimposed on S.P. shifting, there must be a small chemical effect, because the shifts are slightly different: Fe is shifted by 1·0 eV, O by 1·5 eV and Cd by 0·8 eV. These observations could all be reconciled with the hypothesis of poorly crystalline surface compounds of hydroxide type (possibly mixed hydroxide).

Continued cycling increases the intensity ratio of Cd in relation to Fe, suggesting an increasing precipitation of cadmium-containing material on the iron particles. The shape of the iron peak changes in a way which suggests an increasing contribution of divalent iron and a decrease of the three valent state. Only one Cd peak is present with roughly the same position as in the CdO of the uncycled specimen. XRD shows that the dominating crystalline phase after 180 cycles besides α—Fe is $Cd(OH)_2$ and a small amount of metallic cadmium. In the ESCA spectra the metallic state of cadmium does not appear because the metal is covered by oxide or hydroxide. The absence of S.P. shifting of the Cd peak suggests that the grain size of $Cd(OH)_2$ must be very small, and that it must be uniformly distributed on a conducting substrate.

The overall picture that evolves from the results so far presented is that of a gradual covering of the surfaces of both iron and magnetite, probably with a hydroxide in which cadmium is dominant. This layer has poor electron conductivity when first formed, but on continued cycling, the conductivity increases. The formation of this normal layer is disturbed when the electrolyte is allowed to pick up CO_2.

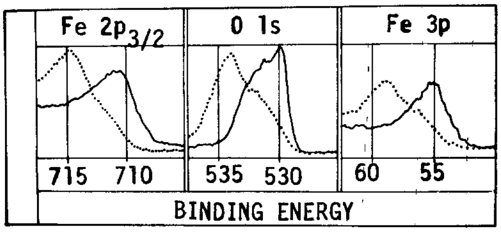

Fig. 10. ESCA spectra of the Cd free electrode after 100 cycles. The dotted peaks are recorded before ion etching.

A few experiments made on a cadmium-free electrode addition may be reported to round off this picture. After 100 cycles, XRD showed small, broad peaks of δ—FeOOH. Fig. 6 shows that the structure has coarsened to 3 μm. The ESCA spectrum after ion milling is shown in Fig. 10. We note that the double oxygen peak and the iron peak both clearly resemble those obtained after 180 cycles in the cadmium-containing electrode. Before ion milling, all the peaks of this spectrum (including the Fe 3p peak not discussed in the earlier spectra) showed a uniform shift towards the high-energy side, indicating that only S.P. effects were active. Since in this case there is no possibility of reaction with another metallic component, only uniform shifts can be expected. The strong S.P. shift observed in the Cd-free electrode

Table 1. The ratio between some characteristic diffraction peaks of Fe_3O_4 and $Cd(OH)_2$ to α—Fe

Number of cycles	Fe_3O_4(4 0 0) α—Fe(1 1 0)	$Cd(OH)_2$(0 0 1) α—Fe(1 1 0)	*Note*
0	0·23	0	CdO (see Fig.7)
6	0·10		Weak peaks of $Cd(OH)_2$
40	0·21	0·10	$CdCO_3$
80	0·10	0·04	$CdCO_3$
100	0·14	0·13	
180	0	0·13	Weak peaks of Cd metal

suggests that the electron conductivity of the surface coating of $\delta-FeOOH$ is poorer than that of the coating developed after long cycling in a Cd-containing electrode.

Acknowledgements

The author is grateful to Svenska Ackumulator AB Jungner of Oskarshamn for the preparation of the samples and to Drs U. Falk, N-E. Barring and S. Landstedt for discussions and to Prof. H. Fischmeister for suggesting this field of study and for continued advice and discussions; further to Mr U. Jelvestam for competent experimental assistance.

References

[1] K. Siegbahn, C. Nordling, A. Fahlman, R. Nordberg, K. Hamrin, J. Hedman, G. Johansson, T. Bergmark, S-E. Karlsson, I. Lindgren and B. Lindberg, ESCA-Atomic, Molecular and Solid State Structure Studied by Means of Electron Spectroscopy. Uppsala 1967 Almquist and Wiksells boktryckeri AB, Uppsala 1967.
[2] S. Landstedt, Jungner, private communication.
[3] I. Olefjord, *Scandinavian Journal of Metallurgy* 3 (1974) 129.